Velocity and Temperature Distribution of Flowing Water in a Solar Parabolic Trough Receiver

Arpakorn Wattana*, Wattanapong Rakwichian, Wannee Ekasilp***, Ammata Tusnapucki******

*Ph.D. Student, School of Renewable Energy Technology (SERT), Naresuan University, Phitsanulok 65000, Thailand
**School of Renewable Energy Technology (SERT), Naresuan University, Phitsanulok 65000, Thailand
**Department of Mechanical Engineering, College of Engineering, Rangsit University, Pathumthani 12000, Thailand
****Department of Mechanical Engineering, Faculty of Engineering, Sripatum University, Bangkok 10900, Thailand
Tel: +66-2997-2222-30, Fax: +66-2533-9470, E-mail: warpakorn@windowslive.com

ABSTRACT

This paper focuses on the determination of the velocity and temperature distribution for water flow in a parabolic trough receiver by using simulation technique. In order to determine the velocity and temperature distribution of water flow through this receiver, the velocity of a normal and parallel direction of water flow, the relationship between the water's mass flow rate and the temperature of water while flowing trough the receiver pipe are determined. The methodology of this study is based on solving partial differential equations by using finite difference method of mass, momentum and energy conservation. This method applies a Power law model to momentum equations and applies a central difference model to energy equation. The set of discretization equations are solved simultaneously by "SIMPLE" algorithm to obtain velocity and temperature distribution within the receiver.

Key Words: *Parabolic trough receiver, Finite difference method, SIMPLE algorithm, Velocity distribution, Temperature distribution.*

Nomenclature

C_P : Constant specific heat, (kJ/kg.K)
f : Focal length, (m)
I_b : Beam radiation on the aperture area, (W/m^2)
k : Thermal conductivity, (W/m.K)
l : Length, (m)
P : Pressure, (kPa)
P^* : Guessed pressure, (kPa)
P' : Pressure correction, (kPa)
S : Absorbed radiation per unit area, (W/m^2)
T : Temperature, (K)
u : Velocity in the axial z direction, (m/s)
u^* : Guessed velocity in the axial z direction, (m/s)
u' : Velocity correction in the axial z direction, (m/s)
v : Velocity in the axial y direction, (m/s)
v^* : Guessed velocity in the axial y direction, (m/s)
v' : Velocity correction in the axial y direction, (m/s)
ρ : Density, (kg/m^3)

μ : Viscosity, (kg/m.s)
$\eta_{o(\mathrm{mod})}(\theta)$: Modified optical coefficient
$K(\theta)_{Duf}$: Incident angle modifier
$\eta_o(\theta)$: Overall optical efficiency
$\xi(\theta)$: End effect correction
θ : Incidence angle, (degrees)
θ_z : Zenith angle, (degrees)
ϕ : Latitude, (degrees)
δ : Declination angle, (degrees)
ω : Hour angle, (degrees)
γ : Intercept factor
ρ_e : Specular reflectance of the concentrator
τ : Transmittance
α : Absorptance

1. INTRODUCTION

In the present, there are different types of solar collectors, such as flat-plate, parabolic trough, parabolic dish, and Fresnel lens. The suitability and economic viability of each of these collectors for an intended application depend on the nominal temperature of the thermal conversion. Suitability of flat-plate collector application for low temperature has been proven worldwide. However, some issues appear when one wants to achieve temperatures that are higher than 150˚C. The first issue is that the solar radiation must be concentrated. The concentration can be made in several ways. The two most common concentration methods are; using a reflecting surface that concentrates the direct solar radiation onto a receiver with an area smaller than the collecting one (this method is applied in parabolic trough collector and parabolic dish) and using Fresnel lenses (consisting of many small refractive surfaces) on absorber tubes [1].

Parabolic trough collector can be operated at temperature up to 450˚C (as the result of the optical concentration affected by parabolic-shaped reflector). The parabolic trough collector therefore suits for medium temperature conversion of solar radiation. Parabolic dishes are paraboloids of revolution (dish-shaped). This method allows a highly concentrated direct solar radiation on the focal point of the parabola. This collector is able to achieve the temperature up to 1100˚C during the operation. The line-focus Fresnel lens collectors can operate up to 300˚C, while point-focus Fresnel lens can operate at temperature over 600˚C. Even though the operated temperature is within the medium temperature range (150-400˚C), Fresnel lens collectors are more expensive than parabolic trough collectors [1]. Parabolic trough collectors (PTCs) are considered the best option at medium temperature range operation.

Parabolic trough collectors are the main technology currently used in solar thermal electric power generation plants. Parabolic trough power plants use concentrated sunlight to provide the thermal energy, required to drive a conventional power plant. These plants use a large field of parabolic trough collectors, which track the sun during the day and concentrate the solar radiation on a receiver pipe, located at the focus of the parabolic shaped mirrors. A working fluid passes through the receiver then it is heated, and becomes steam for driving a conventional Rankine cycle steam power plant.

Most of the published studies of parabolic trough collectors are concerned with the Luz trough collector, which is used for the Solar Thermal Electric Generation Systems (SEGS) plant at Kramer Junction in Southern California. The receiver of the SEGS system consists of a heat absorption steel pipe, coated with a black chrome selective surface or a low thermal emittance cermet selective coating [2].The absorber pipe is covered by an evacuated glass tube, that is coated with anti-reflective coating on both surfaces. Thermal VP-1 is used as the collector heat transfer fluid in SEGS plants. Sandia National Laboratories performed testing on a typical sector of the LS2 SEGS trough

collector for determine the thermal loss and its efficiency. Chrome black and cermet selective coatings were studied together with three receiver configurations; glass envelopes vacuum or air in the receiver annulus and a bare receiver tube [3]. A direct steam generation collector (DSG) has been proposed [2] as a future development of the SEGS trough collector in order to eliminate the costly synthetic oil, intermediate heat transport piping loop and oil to steam heat exchanger. Three concepts for a DSG collector system that have been proposed[4,5] are; the once-through concept to generate superheated stream in one pass, the recirculation process concept to generate wet steam and the injected water system to control steam quality and flow instability along the absorber pipe. Odeh et al, [6] developed an efficiency equation of parabolic trough collectors for Synthetic oil (currently used in LUZ plant) and water operations. A simulation model, linked with the TRNSYS simulation program was used to determine the annual performance of a typical trough configuration under Australian conditions. Jacobson et al, [7] developed a software simulation of a solar parabolic trough to use in the design of a solar thermal power plant. In order to determine the optimum size of a parabolic trough to increase the power of a solar thermal power plant system in Thailand, the simulation was created as a tool to determine the optimum parameters for the parabolic trough. These parameters were input to the power plant. Kim and Seo [8] studied the thermal performance of a glass evacuated tube solar collector, which was numerically and experimentally investigated. The solar collector consisted of a two-layered glass tube and an absorber tube. Air was used as the working fluid. The length and diameter of this glass tube were 1200 and 37 mm respectively. Four different shapes of absorber tubes were considered. The performances of the solar collectors were studied to find the best shape of the absorber tube for the solar collector.

The scope of this paper is to determine temperature and velocity distribution of water flow in a receiver pipe by using finite different method. The velocity at the normal and parallel direction and the relationship between the mass flow rate and the temperature of water flowing in the receiver pipe, will be determined and achieved.

2. PARABOLIC TROUGH COLLECTORS

Parabolic through collectors (PTCs) can effectively produce heat at temperature between 50 and 400°C. PTCs are made of a reflective material sheet which is bent into a parabolic shape. A black metal pipe is placed along the focal line of the receiver pipe. The pipe is covered with a glass tube in order to prevent heat losses, as shown in the Figures 1 and 2.

Fig.1 Parabolic trough collectors field at the Kramer Junction, California [9].

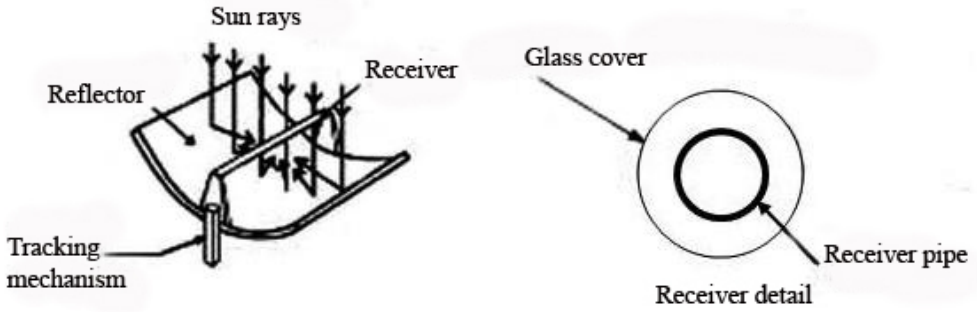

Fig.2 Schematic of a parabolic trough collector [10].

When the parabola is pointed towards the sun, the parallel rays will be incident on the reflector and then reflect onto the receiver pipe. The working fluid then flows through the receiver and absorbs heat. The collector can be oriented in an east–west direction to track the sun towards north/south directions. Also, the collector can be oriented in a north–south direction to track the sun towards east/west directions.

3. ASSUMPTIONS

1. The heat flux is uniform around the circumference and along the length of a receiver pipe.
2. The radiation heat transfer from the collector, the ground and the surrounding trough is negligible.
3. The annulus between the absorber and glass envelope is under vacuum.
4. The heat losses from the receiver pipe are negligible.
5. Fully flowing fluid in the receiver pipe.
6. Incompressible Newtonian fluid.
7. Two-dimensional flow and steady –uniform flow.
8. No-slip boundary condition.
9. The body forces acting on the fluid is negligible.
10. The viscous-energy dissipation is negligible.

4. GOVERNING EQUATIONS

4.1 Absorbed radiation

For a parabolic trough collector, only the direct solar radiation will be obtained for practical use. The following steps were followed using Duffie's and Beckman's[11]. Given that the latitude (ϕ) of Phitsanulok area is 16°, 47' N. All of the modifiers taken into the Absorbed Radiation (S) or the actual amount of radiation on the receiver can be calculated by equation (1):

$$S = I_b * \eta_{o,\mathrm{mod}}(\theta) * \xi(\theta) * \cos\theta \tag{1}$$

where

$$\eta_{o,\mathrm{mod}}(\theta) = K(\theta)_{Duf} * \eta_o(\theta) \tag{1a}$$

$$K_{DUF}(\theta) = 1 - 6.74E^{-5} * \theta^2 + 1.64E^{-6} * \theta^3 - 2.51E^{-8} * \theta^4 \tag{1b}$$

$$\eta_o(\theta) = \rho_e * \gamma * \tau * \alpha \tag{1c}$$

$$\xi(\theta) = 1 - (f/l) * \left(1 + \frac{a^2}{48 * f^2}\right) * \tan(\theta) \tag{1d}$$

$$\cos\theta = (\cos^2(\theta_z) + \cos^2(\delta) * \sin^2(\omega))^{1/2} \tag{1e}$$

$$\cos\theta z_z = \cos(\phi) * \cos(\delta) * \cos(w) + \sin(\phi) * \sin(\delta) \tag{1f}$$

4.2 Equation of motion

In order to determine the velocity distribution in the fluid flow, the equation of motion will be used. The governing equations for incompressible fluid flow are the continuity and momentum equations [12]. The coordinate transformation method is used for converting from Cylindrical coordinates to Cartesian coordinates. The selected cylindrical coordinate systems are $z = z$, $y = r\sin\theta$ and $x = r\cos\theta$, at $\theta = 90^0$ then $z = z, y = r, and\ \ x = 0$, as shown in the Figure 3 :

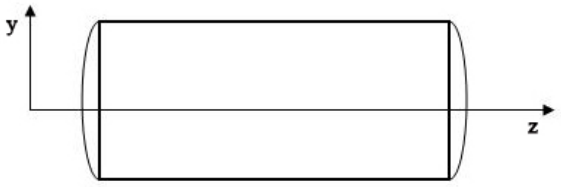

Fig. 3 Cross-section of cylindrical pipe.

Continuity equation

$$\frac{\partial(\rho u)}{\partial y} + \frac{\partial(\rho v)}{\partial z} = 0 \tag{2}$$

Momentum equations

$$z - momentum : \rho\left(\frac{v\partial u}{\partial y} + \frac{u\partial u}{\partial z}\right) = -\frac{\partial P}{\partial z} + \mu\left(\frac{\partial^2 u}{\partial y^2} + \frac{\partial^2 u}{\partial z^2}\right) \tag{3}$$

$$y - momentum : \rho\left(v\frac{\partial v}{\partial y} + u\frac{\partial v}{\partial z}\right) = -\frac{\partial P}{\partial y} + \mu\left(\frac{\partial^2 v}{\partial y^2} + \frac{\partial^2 v}{\partial z^2}\right) \tag{4}$$

4.3 Equation of energy

The temperature distribution in the flow field is governed by the energy equation. This equation is derived by writing an energy balance to the first law of thermodynamics. For a differential volume element in the flow field that is in a form of the Cartesian coordinates could be given by the equation (5):

$$\rho C_P\left(u\frac{\partial T}{\partial z} + \frac{v\partial T}{\partial y}\right) = k\left(\frac{\partial^2 T}{\partial z^2} + \frac{\partial^2 T}{\partial y^2}\right) \tag{5}$$

4.4 Boundary conditions

The boundary conditions are:

$S = q''_{cond} = -KA\dfrac{\Delta T}{\Delta y}$ at the outer surface of a receiver pipe

$z = 0;\ T = T_i$

$u = u_i$

$v = v_i$

$P = P_i$

$z = L;$ Out flow condition

$y = 0;$ Symmetric condition.

$y = R;$ Uniform heat flux.

$u, v = 0$ (No slip condition)

5. FINITE DIFFERENCE SCHEMES

In this study, the author constructed a finite difference scheme in the form of Cartesian Coordinates for the incompressible flow based on equations (2) to (5). These equations can be employed by using Power law model for momentum equations and Central difference model for energy equation.

5.1 Continuity and momentum equations

The continuity equation is discretized at the pressure point, while the components of the momentum equation are discretized at the corresponding velocity points[13]:

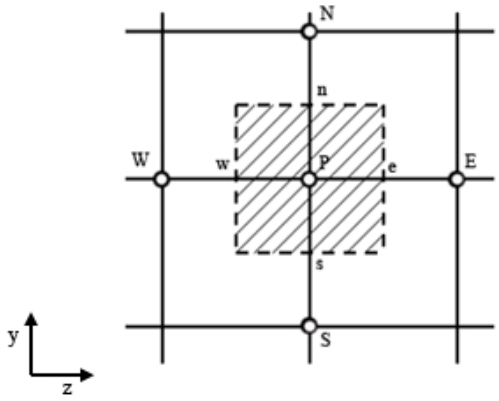

Fig.4 Control volume for the continuity, momentum, and energy equations.

Momentum equations

The two-dimensional discretization equation can now be written as

$$a_P u_P = a_E u_E + a_W u_W + a_N u_N + a_S u_S + (P_P - P_E)\Delta y \quad (6)$$

$$a_P v_P = a_E v_E + a_W v_W + a_N v_N + a_S v_S + (P_P - P_N)\Delta x \quad (7)$$

where

$$a_P = a_E + a_W + a_N + a_S \tag{8}$$

$$a_E = D_e A(|P_e|) + [[-F_e, 0]] \ , \ a_W = D_w A(|P_w|) + [[F_w, 0]] \tag{9}$$

$$a_N = D_n A(|P_n|) + [[-F_n, 0]] \ , \ a_S = D_s A(|P_s|) + [[F_s, 0]] \tag{10}$$

The flow rate and conductances are defined as

$$F_e = (\rho u)_e \Delta y \ ; (\rho u)_e = \frac{(\rho u)_E + (\rho u)_P}{2} \tag{11}$$

$$F_w = (\rho u)_w \Delta y \ ; (\rho u)_w = \frac{(\rho u)_P + (\rho u)_W}{2} \tag{12}$$

$$F_n = (\rho v)_n \Delta z \ ; (\rho v)_n = \frac{(\rho v)_n + (\rho v)_P}{2} \tag{13}$$

$$F_s = (\rho v)_s \Delta z \ ; (\rho v)_s = \frac{(\rho v)_P + (\rho v)_S}{2} \tag{14}$$

$$D_e = \frac{\mu_e \Delta y}{\Delta z} \ , \ D_w = \frac{\mu_w \Delta y}{\Delta z} \ , \ D_n = \frac{\mu_n \Delta z}{\Delta y} \ , \ D_s = \frac{\mu_s \Delta z}{\Delta y} \tag{15}$$

Assumption $\mu_e = \mu_w = \mu_n = \mu_s =$ Constant viscosity

And the Peclet number are defined by

$$P_e = \frac{F_e}{D_e} \ , \ P_w = \frac{F_w}{D_w} \ , \ P_n = \frac{F_n}{D_n} \ , \ P_s = \frac{F_s}{D_s} \tag{16}$$

The Power law scheme is recommended, which

$$A(|P|) = [[0, (1 - 0.1|P|)^5]] \tag{17}$$

then

$$A(|P_e|) = [[0, (1 - 0.1|P_e|)^5]] \ , \ A(|P_w|) = [[0, (1 - 0.1|P_w|)^5]] \tag{18}$$

$$A(|P_n|) = [[0, (1 - 0.1|P_n|)^5]] \ , \ A(|P_s|) = [[0, (1 - 0.1|P_s|)^5]] \tag{19}$$

The pressure and velocity corrections

The aim is to improve the guessed pressure P^* to satisfy the continuity equation. The author therefore determined a relationship between the velocity components and pressure change rate.

The corresponding velocity correction (u', v') can then be introduced in a similar manner. Equation (20) shows the correct pressure, while the equation (21) and (22) show correct velocity as presented in [13].

$$P = P^* + P' \tag{20}$$

$$u = u^* + u' \tag{21}$$

$$v = v^* + v' \tag{22}$$

The pressure-correction equation

The two-dimensional discretization equation for the pressure-correction equation can now be written as;

$$a_{PP}P_P^{'} = a_{EE}P_E^{'} + a_{WW}P_W^{'} + a_{NN}P_N^{'} + a_{SS}P_S^{'} + b \tag{23}$$

where

$$a_{PP} = a_{EE} + a_{WW} + a_{NN} + a_{SS} \tag{24}$$

$$a_{EE} = \rho_E\left(\frac{\Delta y}{a_E}\right)\Delta y \ , \ a_{WW} = \rho_W\left(\frac{\Delta y}{a_W}\right)\Delta y \tag{25}$$

$$a_{NN} = \rho_N\left(\frac{\Delta z}{a_N}\right)\Delta z \ , \ a_{SS} = \rho_S\left(\frac{\Delta z}{a_S}\right)\Delta z \tag{26}$$

$$b = \left[\left(\rho u^*\right)_W - \left(\rho u^*\right)_E\right]\Delta y + \left[\left(\rho v^*\right)_S - \left(\rho v^*\right)_N\right]\Delta z \tag{27}$$

5.2 Energy equation

The two-dimensional discretization equation for the energy equation can now be written as

$$a_P T_P = a_N T_N + a_S T_S + a_E T_E + a_W T_W \tag{28}$$

where

$$a_P = \frac{2k}{\Delta y^2} + \frac{2k}{\Delta z^2} \ , \quad a_N = \frac{k}{\Delta y^2} - \frac{\rho C_P v_P}{2\Delta y} \tag{29}$$

$$a_S = \frac{k}{\Delta y^2} + \frac{\rho C_P v_P}{2\Delta y} \ , \quad a_E = \frac{k}{\Delta z^2} - \frac{\rho C_P u_P}{2\Delta z} \tag{30}$$

$$a_W = \frac{k}{\Delta z^2} + \frac{\rho C_P u_P}{2\Delta z} \tag{31}$$

6. THE SIMPLE ALGORITHM

SIMPLE, which stands for Semi-Implicit Method for Pressure-Linked Equations, has been employed in this research to simulate the flow field. The algorithm has been described in [13], as following steps;

1. Guess the pressure field P^* as an initial input.
2. Solve the momentum equations to obtain velocity u^* and v^*.
3. Solve the $P^{'}$ equation.
4. Calculate value P by adding value $P^{'}$ to P^*.
5. Calculate velocity u and v from their previous values using the velocity-correction formula.
6. Solve the discretization equation for the other $\phi^{'}s$ (such as temperature, concentration and turbulence quantities), if they influence the flow field through fluid properties, source terms, and etc.(If a particular ϕ does not influence the flow field, it is recommended to determine after a converged solution, for the flow field has been obtained.)
7. Treat the corrected pressure P as a new guessed pressure P^*, then return to step 2 and repeat the whole procedure until a converged solution is obtained.

7. RESULTS AND DISCUSSION

Table 1 shows an input parameter for the simulation.

Table 1 Input parameters

Solar radiation	
Latitude(Phitsanulok province, degree)	16.75
Day of the year	152
Parabolic trough concentrator, orientated in a north–south direction.	
Aperture width (m)	5.77
Module length (m)	12.50
Focal length (m)	1.71
Specular reflectance	0.90
Receiver pipe	
Cover diameter (m)	0.09
Outer diameter (m)	0.07
Inner diameter (m)	0.066
Absorber length (m)	12.5
Intercept factor	1
Thermal conductivity (W/m.K)	47.6
Specular absorbance	0.93
Cover transmittance	0.82
Cover thickness (m)	0.0025
Cover extinction coefficient (m^{-1})	32
Cover refractive index	1.526
Working fluid(water) conditions	
Inlet temperature (K)	303.15
Inlet pressure (MPa)	1.013
I Mass flow rate (kg/s)	0.03
II Mass flow rate (kg/s)	0.05
III Mass flow rate (kg/s)	0.30

The simulation was conducted on May 31st, 2008 from 8.03 a.m. to 5.03 p.m. at Phitsanulok province by School of Renewable Energy Technology (SERT), Naresuan University, Thailand (the solar radiation data, used in the simulation were measured by SERT). The results are carried out for water flow in parabolic trough receiver, which are presented in Figures 5 to 11. Figure 5 shows beam radiation and heat flux on aperture area of parabolic trough collector at Phitsanulok province. Figure 6 to 8 show the temperature distribution in the receiver. Figure 9 and 10 show the velocity distribution in the receiver. The pressure in the receiver is shown in the Figure 11.

7.1 Temperature distribution

The results in Figure 5 reveal that the average beam radiation is 282.38 W/m^2, while the maximum beam radiation is 517.09 W/m^2 at 11.23 a.m. The average heat flux on the aperture area is 166.38 W/m^2, while the maximum heat flux is 305.99 W/m^2. Figure 6 shows the average outer surface temperature of the receiver pipe, the average water temperature in the receiver, and the outlet water temperature at the exit of a receiver pipe at the mass flow rate is equal to 0.03 kg/s. The maximum temperature of outer surface is 535.64 K at 11.23 a.m. The maximum average water temperature in

the receiver is 377.35 K at 11.23 a.m. and the maximum outlet temperature at the exit of receiver is 461.33 K at 11.23 a.m.

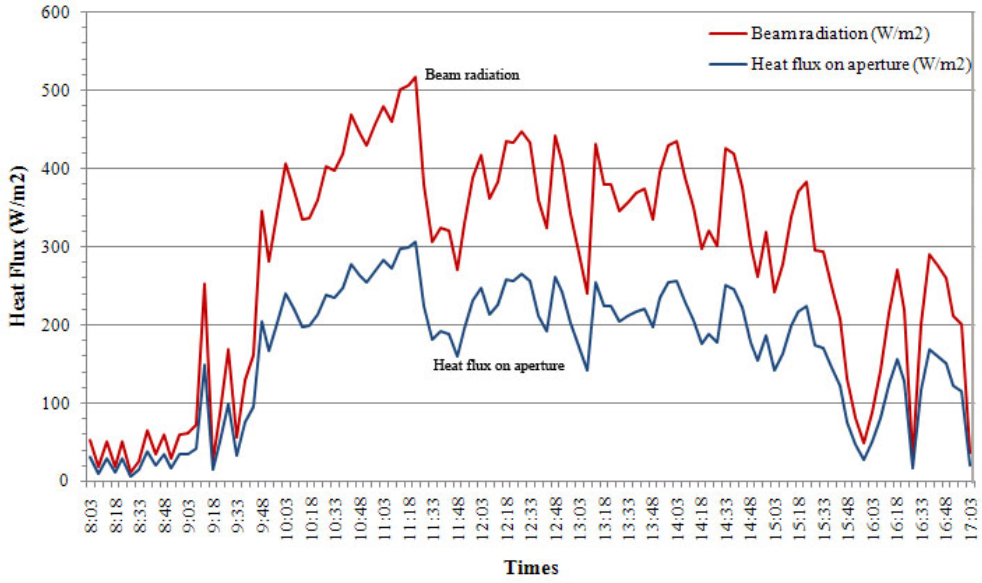

Fig.5 Beam radiation at Phitsanulok province.

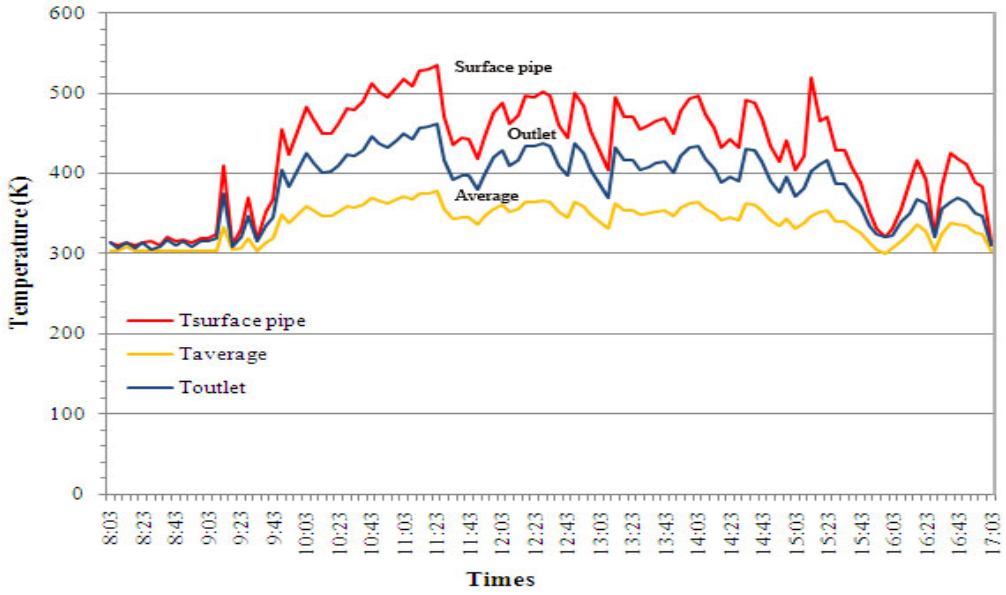

Fig. 6 Temperature distribution in a receiver pipe as the mass flow rate is equals to 0.03 kg/s.

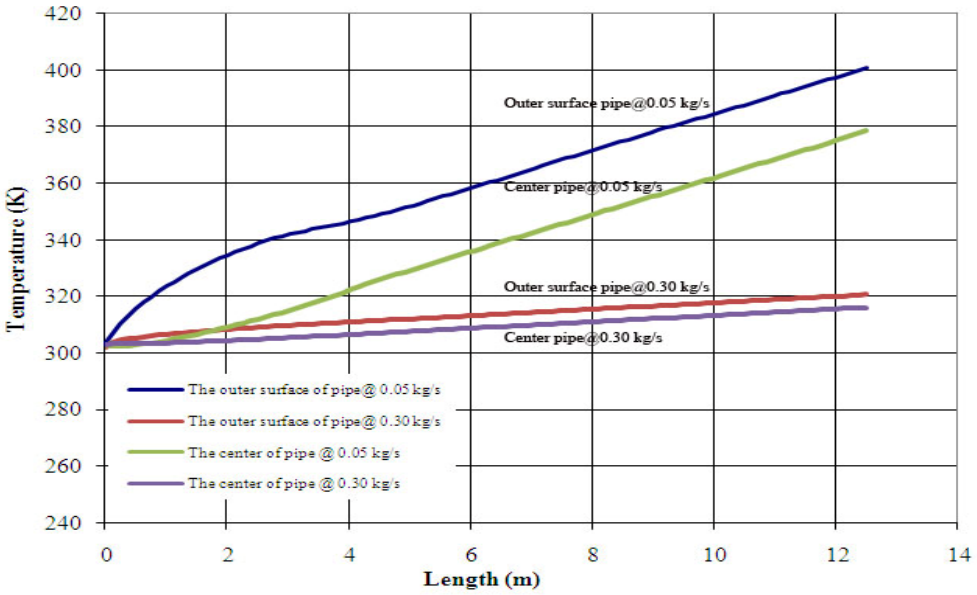

Fig. 7 Temperature throughout the position of a receiver pipe at 12.03 p.m., as the mass flow rate is equals to 0.05 kg/s and 0.3 kg/s respectively.

From Figure7, it is found that the temperature of a receiver pipe at the mass flow rate of 0.05 kg/s are higher than that of mass flow rate 0.30 kg/s. The maximum temperature is at the exit position, e.g. at the mass rates of 0.05 kg/s and 0.3 kg/s, the outer surface temperatures and the temperature at the pipe center are 400.85 K, 378.54 K, and 320.60 K, respectively.

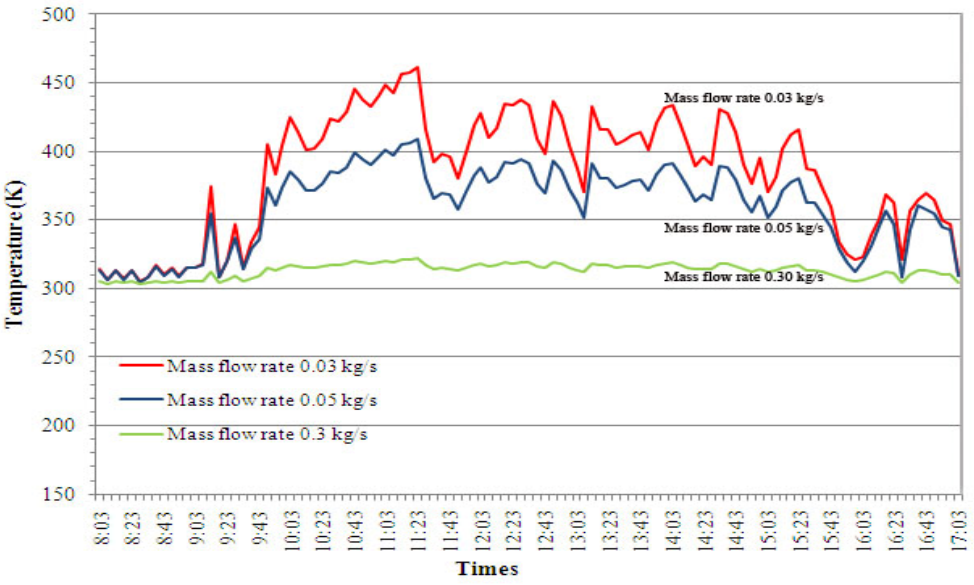

Fig. 8 Temperature of the water at exit position of a receiver pipe as the mass flow rate is equal to 0.03, 0.05 and 0.3 kg/s respectively.

Figure 8 shows the temperature of the water at the exit position of a receiver pipe, for the mass flow rate of 0.03, 0.05, and 0.3 kg/s at 11.23 a.m., the maximum temperatures are 581.74 K, 412.91 K and 321.66 K, respectively. At the mass flow rate of 0.3 kg/s data, the water temperature at the exit position of the receiver pipe is lower than of mass flow rate 0.03 and 0.05 kg/s data. This

reveals that if the flow rate is higher, the heat transfer from the pipe surface to the flowing water will be lower.

From the simulation, it can be summarized that the temperature curve is instable due to the heat flux, entering the receiver pipe is uncontrollable.

7.2 Velocity distribution

Figure 9 to 10 show the velocity distribution of water flow in the receiver pipe, when the mass flow rate is equal to 0.03 kg/s, 0.05 kg/s and 0.30 kg/s respectively at 12.03 p.m. The graphs are shown in the z-axis direction and y-axis direction, located at the center of pipe position. The results in Figure 9 reveal that the z-velocity of water flows in a receiver pipe. (as shown in Figures 9(a) to 9(d).) explores the mass flow rate at 0.03 kg/s, giving the average velocity is 0.040 m/s, the maximum velocity is 0.041 m/s (at position 3.66 meter of pipe length) and the minimum velocity is 0.039 m/s (at position 1.26 meter of pipe length). As the mass flow rate is equal to 0.05 kg/s, the average velocity is 0.061 m/s, the maximum velocity is 0.622 m/s (at position 12.49 meter of pipe length), and the minimum velocity is 0.059 m/s (at position 1.27 meter of pipe length). For the mass flow rate equal to 0.30 kg/s, the average velocity is 0.357 m/s, the maximum velocity is 0.358 m/s (at position 12.49 meter of pipe length), and the minimum velocity is 0.354 m/s (at position 0.64 meter of pipe length). Throughout a receiver pipe position, z-velocity is rather stable, shown in the Figure 9(d). The results in Figures 10(a) and 10(b) reveal that the y-velocity of water flows in a receiver pipe, for the mass flow rate equal to 0.03 kg/s, at the center of pipe position, the average velocity is given 2.939×10^{-8} m/s, at position 0.2 mm from the inner surface of pipe, the average velocity is 3.29×10^{-7} m/s. For the mass flow rate of 0.05 kg/s and 0.30kg/s, the average velocity are 9.051×10^{-8} m/s and 1.064×10^{-6} m/s, respectively.

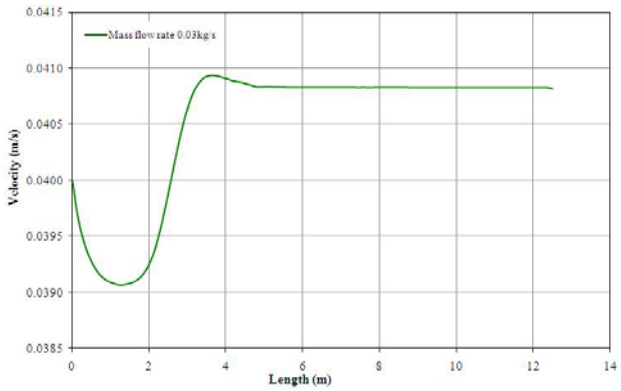

(a) Mass flow rate 0.03 kg/s

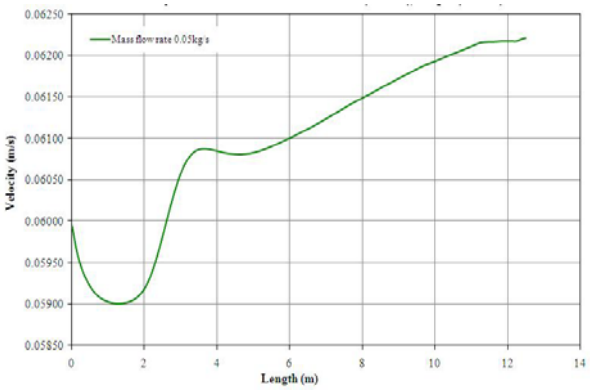

(b) Mass flow rate 0.05 kg/s

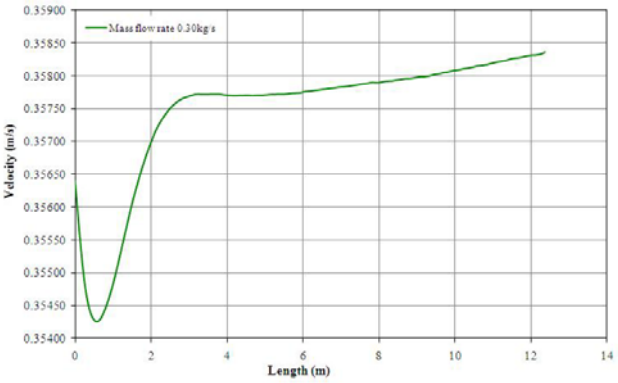

(C) Mass flow rate 0.3 kg/s

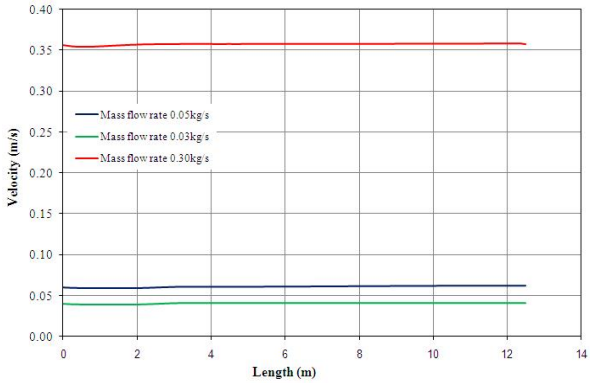

(d) Mass flow rate 0.03, 0.05 and 0.3 kg/s

Fig.9 Velocity distribution of water flows in a receiver pipe in Z-direction at 12.03 p.m.

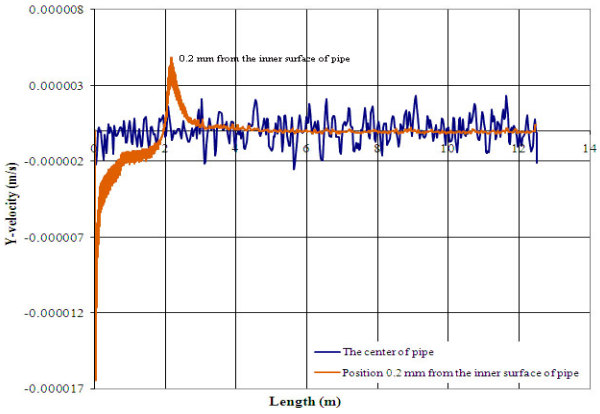

(a) Mass flow rate 0.03 kg/s

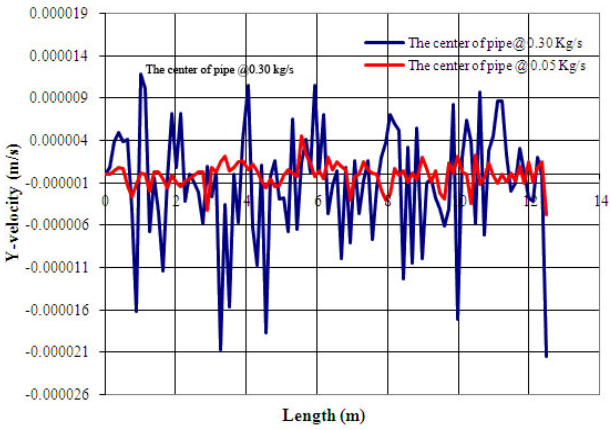

(b) Mass flow rate 0.05 and 0.3 kg/s

Fig. 10 Velocity distribution of water flows in a receiver pipe in y-direction at 12.03 p.m.

The simulation shows that the velocity of water flow in a receiver pipe in z-direction, 4 m pipe length from the entrance, the flowing water in the pipe is expectedly found to be instable. After the water has been heated, the water flow rate is stabilized and become steady. From the results, velocities of water flow in the y-direction are slightly changed through the pipe length.

7.3 Pressure in the receiver

Figure 11 shows the total pressure through the whole length of a receiver pipe at 12.03 p.m. At the mass flow rate of 0.03 kg/s, 0.05 kg/s and 0.30 kg/s, the total pressure at the entrance pipe are 1013.25 kPa and the total pressure at the exit pipe are 1011.72 kPa, 1009.79 kPa and 914.76 kPa respectively. The results in Figure 11 reveal that the small pressure drops within the receiver pipe.

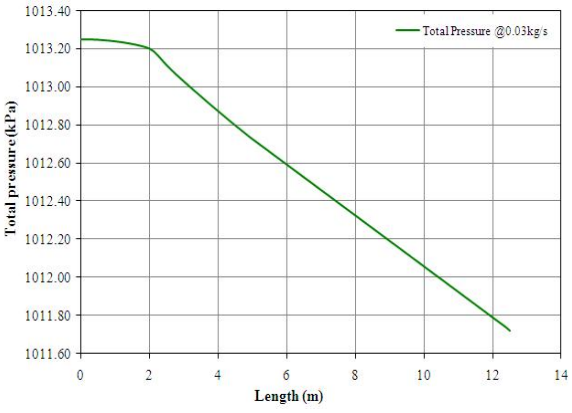

(a) Mass flow rate 0.03 kg/s

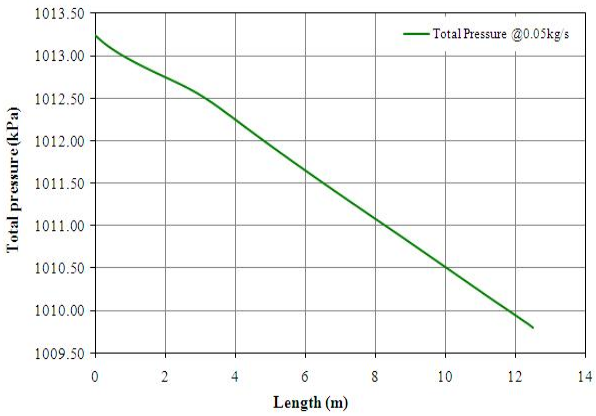

(b) Mass flow rate 0.05 kg/s

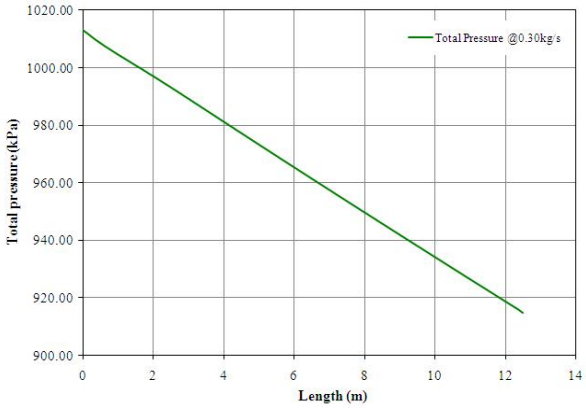

(c) Mass flow rate 0.3 kg/s

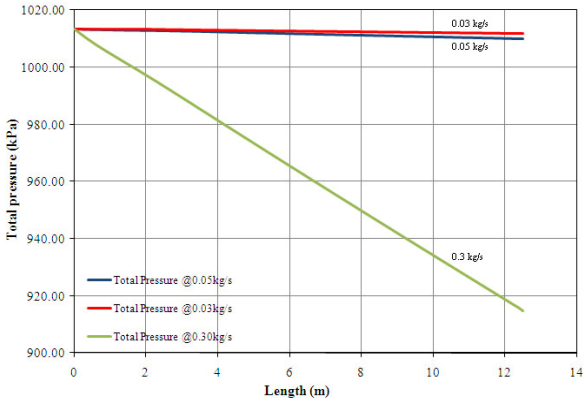

d) Mass flow rate 0.05, 0.03 and 0.3 kg/s

Fig.11 The total pressure within a receiver pipe at 12.03 p.m.

8. CONCLUSIONS

The result from the simulation can be summarized that the velocity of water flows in a receiver pipe is rarely changed, unless the range of a pipe length is adjusted between 0 to 3 meters. This range is an adaptation of fluid movement after the water has been heated and the pressure drop within the receiver pipe, the pressure drop is rather small. Additionally, the study also found that the heat flux on the aperture area of parabolic trough collector is inconstant because of an inconstant amount of the beam radiation each day, thereby the temperature of water mass flow rates is considered in this study. At the exit end of the receiver pipe, the temperature fluctuation in each period is diminished if the water mass flow rates are augmented. The inferiority, however, is that if the water mass flow rate increases then the water temperature would be decreased. Thus, if we can reduce the temperature fluctuation, the flowing water temperature of the exit end of a receiver pipe will not decrease. This would be very useful to apply further in thermal technologies. It would also improve a performance of parabolic trough receiver.

.

Acknowledgement

The grateful thanks to a supervisor, Assoc.Prof.Dr.Wattanapong Rakwichian,co- supervisor, Dr. Wannee Ekasilp and Dr. Ammata Tusnapucki, for useful and valuable guidances, suggestions and encouragements throughout this study.

Special thanks are due to staffs of School of Renewable Energy Technology (SERT), Naresuan University, Thailand.

References

[1] Eduardo Z. M.(2004). *Renewable Energy Systems.*centro de Investigaciones Energeticas Medioambientales y Techologicas(IEMAT).

[2] Cohen G. and Kearney D.(1994).*Improved Parabolic Trough Solar Electric System based on the SEGS Experence.* Proceeding of the ASES Annual Conference Solar, 94,147-150.

[3] Dudey V.,Kolb G., Sloan M. and Kearney D. (1994). *SEGS LS2 Solar Collector Test Results.* Report of Sandia National Laboratories, SANDIA U.S.A.,94-1884.

[4] Dagan E., Muller M. and Lippke F.(1992). *Direct Steam Generation in the Parabolic Trough Collector.* Report of Plantaform Solar de Almeria, Madrid.

[5] Lippke F. (1996). *Direct Steam Generation in the Parabolic Trough Solar Power Plants.- Numerial investigation of the Transient and the Control of a Once- Trough System.* Solar Energy Eng.118,9-14.

[6] Odeh S. D., Morrison G.L. and Behnia M.(1996). *Thermal Analysis of Parabolic Solar Collector for Electric Power Generation.* Proceeding of ANZSES 34th Annual Conference, Darwin , Australia, 460-467.

[7] Jacobson E.,Ketjoy N., Nathakgranakule S.,and Rakwichian W. (2006). *Solar Parabolic Trough Simulation and Application for a Hybrid Power Plant in Thailand.* ScienceAsia, 32,187-199.

[8] Kim Y.and Seo T.(2007). *Thermal Performances Comparisons of the Glass evacuated tube Solar Collectors with Shapes of Absorber tube.* Renewable Energy,32,772-795.

[9] Trieb, F., Nitsch, J., Kronshage, S., Schilling, C., and Brischke, L.A.(2002).*Sustainable Energy Supply using Large Scale Solar Thermal Power Plants.* EUROMED 2002,Sinal, Egypt, 4-7.

[10] Soteris, A. K. (2004). *Solar Thermal Collectors and Applications.* Progress in Energy and Combustion Science, 30, 231-295.

[11] Duffie, A. J., and Beckman, A. W. (1991). *Solar Engineering of Thermal Processes.* 2nd ed. New York: John Wiley & Sons.

[12] Ozisik, M. N. (1985). *Heat Transfer A Basic Approach.* International Editions, Mechanical Engineering series, New York: McGraw-Hill.

[13] Suhas V. Patankar. (1980). *Numerical Heat Transfer and Fluid Flow.*Taylor &Francis.